



LBNL-41796  
LSBL-459  
Preprint

# ERNEST ORLANDO LAWRENCE BERKELEY NATIONAL LABORATORY

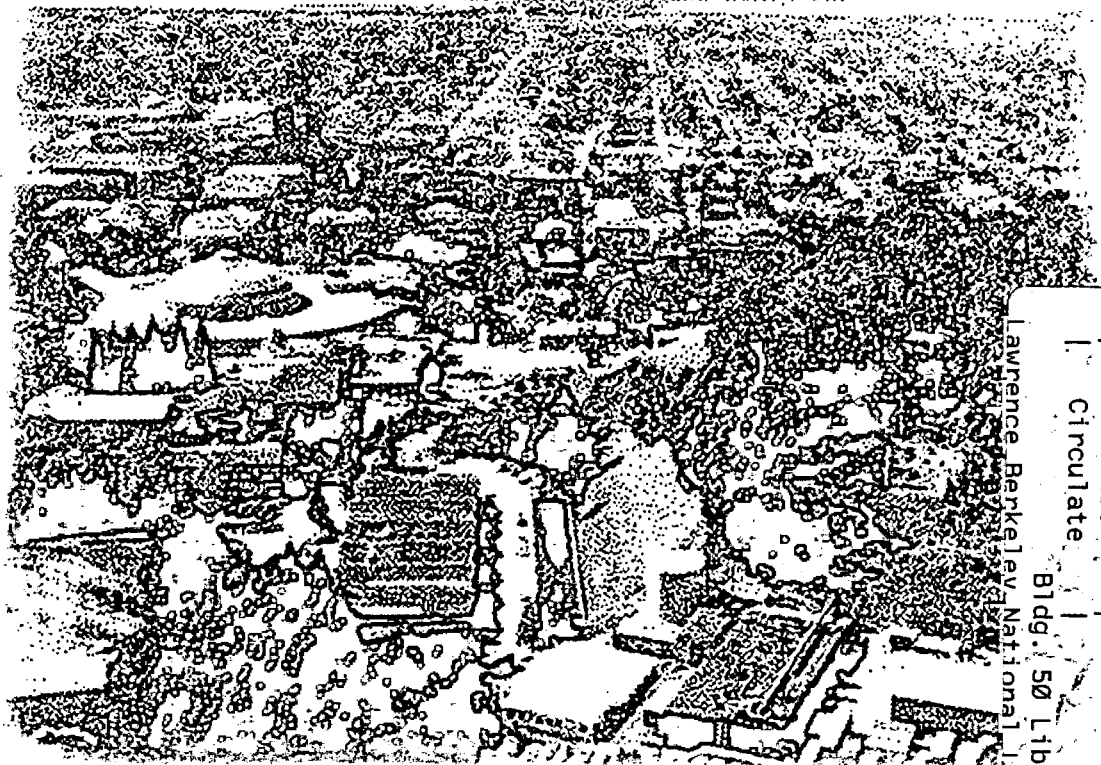
## Imaging Spectroscopic Analysis at the Advanced Light Source

T. Warwick, S. Anders, Z. Hussain, G.M. Lambie,  
G.F. Lorusso, A.A. MacDowell, M.C. Martin,  
S.A. McHugo, W.R. McKinney, and H.A. Padmore

**Advanced Light Source Division**

May 1998

Submitted to  
*Synchrotron Radiation News*



Lawrence Berkeley National Laboratory  
Bldg. 50 Library - Ref.

REFERENCE COPY	_____
Does Not Circulate	_____
Copy 1	_____

LBNL-41796

## **DISCLAIMER**

This document was prepared as an account of work sponsored by the United States Government. While this document is believed to contain correct information, neither the United States Government nor any agency thereof, nor the Regents of the University of California, nor any of their employees, makes any warranty, express or implied, or assumes any legal responsibility for the accuracy, completeness, or usefulness of any information, apparatus, product, or process disclosed, or represents that its use would not infringe privately owned rights. Reference herein to any specific commercial product, process, or service by its trade name, trademark, manufacturer, or otherwise, does not necessarily constitute or imply its endorsement, recommendation, or favoring by the United States Government or any agency thereof, or the Regents of the University of California. The views and opinions of authors expressed herein do not necessarily state or reflect those of the United States Government or any agency thereof or the Regents of the University of California.

## **Imaging Spectroscopic Analysis at the Advanced Light Source**

T. Warwick, S. Anders, Z. Hussain, G.M. Lamble\*, G.F. Lorusso, A.A. MacDowell,  
M.C. Martin, S.A. McHugo, W.R. McKinney, and H.A. Padmore

Advanced Light Source, Ernest Orlando Lawrence Berkeley National Laboratory,  
University of California, Berkeley, California 94720, U.S.A.

\*Center of X-ray Lithography, University of Wisconsin, Madison, Wisconsin, U.S.A.

Submitted for publication to Synchrotron Radiation News

Light Source Note:	
Author(s) Initials	<u>AW</u>
Group Leader's Initials	<u>MRP</u>
Date	<u>5/1/98</u>
Date	

LSBL-459

## Imaging Spectroscopic Analysis at the Advanced Light Source

T. Warwick, S. Anders, Z. Hussain, G. M. Lambie, G. F. Lorusso\*, A. A. MacDowell, M. C. Martin, S. A. McHugo, W. R. McKinney and H. A. Padmore

Lawrence Berkeley National Laboratory, Berkeley, CA94720, USA.

\*Center of X-ray Lithography, University of Wisconsin, Madison, Wisconsin

### Introduction

One of the major advances at the high brightness third generation synchrotrons is the dramatic improvement of imaging capability. There is a large multi-disciplinary effort underway at the ALS to develop imaging x-ray, UV and Infra-red spectroscopic analysis on a spatial scale from a few microns to 10 nm. These developments make use of Infra-red light, Ultra-violet light and x-rays from 100 eV to 10 keV. Imaging and spectroscopy are finding applications to problems in surface science, bulk materials analysis, semiconductor structures, particulate contaminants, magnetic thin films, biology and environmental science.

This article is an overview and status report from the developers of these techniques at the ALS.

### PEEM Microscopy at the ALS

Photoemission electron microscopy (PEEM) using x-rays is a full-field imaging technique based on the secondary electron emission caused by x-ray radiation and absorption. The secondary electrons are imaged by an electron optics column with a resolution given by the electron optics. By varying the incident x-ray wave length incrementally one is able to obtain local Near Edge X-ray Absorption Spectroscopy (NEXAFS) data with high spatial resolution.

There are two PEEM microscopes in operation at the ALS at the moment. The first one, called PRISM, is a two-lens system with a movable aperture in the backfocal plane of the objective lens. The electron optics has a spatial resolution of 200 nm. The microscope is described in detail elsewhere [1]. It is located at beamline 8.0, an undulator beamline with an energy range of 200-1500 eV and a resolving power of  $E/DE = 10000$ . The x-rays are focused on the sample by a Kirkpatrick-Baez pair of mirrors into a spot of 200 nm diameter.

A wide variety of materials and systems have been studied using this microscope including polymers, diamond-like carbon and diamond, various phases of titanium disilicide and of boron nitride, small particles, electron field emission materials, and ceramics (metal nitrides and oxides). In the following, a few examples will be given:

Polymers are very suitable systems for x-ray microscopy studies because the K edges of the elements typically present in polymers (C, N, O, F, Br...) show very strong, sharp, and characteristic resonances for determining the chemical bonding states of the elements [2]. Polymers are used in many technological applications such as colloid paint systems, thin films for the alignment of liquid crystals in liquid crystal displays, lubricants on hard disks, photoresist, to name only those applications we have studied so far. We have studied bilayer systems of polystyrene (PS) and brominated polystyrene (PBrS) consisting of a 30 nm thick PBrS layer on top of a 30 nm thick PS layer produced by spin casting [3]. The samples were annealed for various durations at 180 deg C and studied by scanning transmission electron microscopy (STXM) and PEEM. The formation of spines

as a result of the dewetting process of the two polymers was observed with both methods. STXM was used to identify that the spines are composed of brominated polystyrene. The PEEM results showed that the dewetting of the PBrS starts in small areas exposing the PS underlayer, and in the later phase leads to a complete coverage of the surface with a thin PS film including the PBrS spines. Figure 1 shows a PEEM image of a sample which was annealed for 4 days.

In another series of experiments the tribo-chemical behavior of lubricants on hard disks after wear and the transport of lubricants to the slider surface was studied [4]. It was found that the perfluoropolyether lubricant on the disk undergoes chemical changes during the wear. Fluorine is removed from the polymer, and oxidation in the form of carboxylic bonds takes place. Local NEXAFS spectra taken in wear tracks and on slider surfaces showed that this degraded lubricant is present in wear tracks, but it is also transferred to slider surfaces and accumulated in particular in scratches at the slider.

The new microscope PEEM2 is installed at the bending magnet beamline 7.3.1.1, which provides soft x-rays in the energy range from 250-1500 eV with a resolving power of  $E/DE = 1800$ . Figure 2 shows a schematic of the beamline. The x-rays are focused to a 30 mm spot on the sample. The beamline was designed specifically for XMCD experiments and is equipped with a mask and chopper to select above-plane and below-plane radiation (left and right circular polarized) and in plane radiation (linear polarized). The microscope has been developed to study mainly magnetic materials using X-ray Magnetic Circular Dichroism (XMCD) at high resolution. The electron optics of the microscope consists of an electrostatic system of four lenses, a stigmator, and two deflectors to correct for misalignment. The elements of the electron optics column are shown in Figure 3. The operation voltage is 30 kV. In situ heating up to 1500 deg C and evaporation is possible. An automated sample transfer system allows fast sample exchange, and a sample preparation chamber is equipped with a sputter gun, a heater, and evaporators. The PEEM2 is currently in the commissioning phase. First images have been acquired, and elemental and magnetic contrast has been demonstrated. The calculated resolution limit of PEEM2 is 20-30 nm.

Figure 1. PEEM image of bilayer of PS and PBrS after 4 days of annealing at 180 deg C. Image was acquired at 286.3 eV. The contrast is due to topography, since in the later phase of dewetting the surface is covered completely by PS.

Figure 2. Schematic layout of beamline 7.3.1.1. at the ALS.

Figure 3. Schematic layout of PEEM2. Part of the lens design was adapted from an existing X-ray transmission microscope [5].

ALS contact sanders@lbl.gov

[0] PRISM was built by B. Tonner and G. Castro, PEEM2 by S. Anders, M. Scheinfein, H. A. Padmore and J. Stöhr.

[1] B. P. Tonner, D. Dunham, T. Droubay, and M. Pauli, *J. Electron Spectrosc. Relat. Phenom.* 84 (1997) 211. [2] J. Stöhr, *NEXAFS Spectroscopy*, Springer Verlag, New York, 1992.

[3] These experiments were performed by S. Anders and Th. Stämmler (ALS), H. Ade (North Carolina State University), D. Slep (Hilord Chemical Corp.), J. Sokolov and M. Rafailovich (SUNY@Stony Brook), J. Stöhr (IBM), and C. Heske (ALS)

[4] S. Anders, Th. Stämmler, C. S. Bhatia, J. Stöhr, W. Fong, C.-Y. Chen, and D. B. Bogy, *Materials Research Society Spring Meeting*, San Francisco 1998, to be published.

[5] R. N. Watts, S. Liang, Z. H. Levine, T. B. Lucatorto, F. Polack, and M. R. Scheinfein, *Rev. Sci. Instrum.* 68 (1997) 3464.

## Scanning Zone Plate Microscopes for sub-micron NEXAFS and XPS

Two scanning zone plate microscopes have been developed for x-ray spectroscopic analysis of materials [1], [2]. These instruments operate in tandem at undulator beamline 7.0 at the ALS. A focused x-ray spot is rastered over the sample to make an image, then held on a feature of interest for spectral measurements. The count rates in these microscopes are about ten times higher than previously available. We are presently using zone-plate lenses with a central stop and 80 nm outer zone width, and a corresponding diffraction limit to the spatial resolution of about 100 nm. An order sorting aperture (OSA) is held in front of the sample and precisely positioned on the optical axis ( $\pm 2$  microns) to allow only the first order diffracted focus to reach the sample. The measured FWHM of the x-ray spot is 130 nm.

The Scanning Transmission X-ray Microscope (STXM) provides imaging NEXAFS analysis of samples in transmission at atmospheric pressure. The transmission geometry is the most efficient use of photons for an absorption spectrum, well suited to radiation-sensitive organic samples [3]. Measurements in transmission are bulk sensitive, so that surface contamination is not a concern; this allows the operation of the microscope at atmospheric pressure, in air or helium, with hydrated samples for problems in environmental science [4], [5]. Circularly polarized photons have been generated and used for imaging domains at the L edge in Fe, Ni and Co magnetic films [6]. We have measured  $2 \times 10^7$  photons/second with a spectral width 1/3000 in the zone plate first order focus spot at 300 eV, with the storage ring running at 1.5 GeV, 400 mA. Figure 4. shows a case study illustrating the capability of STXM to perform polarization-sensitive spectromicroscopy of organic polymers at the K edge of the three most important atomic species, C, N and O.

The Scanning Photo-Electron Microscope (SPEM) provides imaging XPS and NEXAFS analysis of sample surfaces in a UHV environment. Here the sample is stationary during imaging and the zone plate is rastered in the illumination field to carry the focused spot across the sample surface. The illumination is of the order of 1mm diameter and the raster range is 80 x 80 microns. The electron spectrometer can view the entire range of the image area, and collects photo-electrons at 60 degrees from the sample normal. The OSA is within 0.5 mm of the sample surface, and the zone plate assembly is cut back on one side to allow a line of sight for the spectrometer. NEXAFS capability is included by means of a UHV flexure to carry the zone plate 0.5mm longitudinally to retain the focus condition as the photon energy changes. The OSA is fixed to the zone plate, with the focal length built into the assembly. Different photon energies require different zone-plate/OSA combinations with different built-in focal lengths (e.g. 700 eV for survey spectra including oxygen 1s photoelectrons, 270 eV to 310 eV for carbon K edge NEXAFS measurements). Five zone plates will be mounted together on a monolithic array with precisely parallel optical axes (to  $\pm 1$ mrad), interchangeable under computer control. So far we have operated the microscope with three zone-plate/OSAs aligned in this way. SPEM allows us to perform quantitative XPS measurements of atomic concentration and core level chemical shifts over regions of the sample surface as small as the spatial resolution of the zone plate lens. The zone plate array can be lowered out of the beam and the sample surface can be observed with a magnifying video system, allowing visible fiducial marks on the sample to be used to position the region of interest within the 100 x 100 micron range of the scan stage. XPS spectra are measured with typical photo-peak count-rates of 70,000 counts/second (Au 4f at 420 eV photon energy).

Figure 4. A sectioned Kevlar fiber measured in STXM (results courtesy of H. Ade and A. Garcia). Absorption spectra are measured at points A and B, showing the dependence on the angle between the photon polarization vector (horizontal) and the preferentially tangential orientation of the pi bonds of N and O. The polarization contrast reverses between the pi and sigma orbital peaks.

Figure 5. A SPEM case study in which an Al/Ti melt has been allowed to solidify on a graphite substrate (results courtesy S. Seal and N. Sobczak). The image of the polished section shows the aluminum metal, precipitates of Al<sub>3</sub>Ti alloy and the graphite interface, with carbide formation. Different core level chemical shifts are observed from the Al, the Al<sub>3</sub>Ti alloy and the carbide region. In this case sputtering has removed the adventitious carbon contamination but the surface is still oxidized.

ALS contact: warwick@lbl.gov

[1] This program originated with a proposal from B. Tonner, Univ. Wisconsin et. al. with continuing development by the ALS.

[2] T. Warwick, H. Ade, S. Cerasari, J. Denlinger, K. Franck, A. Garcia, S. Hayakawa, A. Hitchcock, J. Kikuma, J. Kortright, G. Meigs, M. Moronne, S. Myneni, E. Rightor, E. Rotenberg, S. Seal, H.-J. Shin, R. Steele, T. Tyliczszak and B. Tonner  
J. Synchrotron Rad. 5 (1998) to be published

[3] E.G. Rightor, A.P. Hitchcock, H. Ade, R.D. Leapman, S.G. Urquhart, A.P. Smith, G. Mitchell, D. Fischer, H.J. Shin and T. Warwick  
J. Phys. Chem. B 101(1997)1950

[4] S. C. B. Myneni, J. T. Brown, W. Meyer-Ilse, G. A. Martinez, A. Garcia and A. Warwick

Abstracts of the AGU National Meeting, San Francisco, 1997

[5] T. Grundl, S. Cerasari, A. Garcia, T. Warwick, H. Ade and B.P Tonner  
Compendium of User Abstracts and Technical Reports 1993-1996, LBNL-39981 (1997)

[6] J. Kortright, S.K. Kim, T. Warwick and N.V. Smith  
Appl. Phys. Lett. 71(1997) 1446

### Micro X-ray Photoelectron Spectroscopy on Beamline 7.3.1.2

The Micro XPS beamline has been developed at the Advanced Light Source (ALS), in collaboration with Intel Corporation and Applied Materials, to fulfill the increasingly demanding needs of the semiconductor industry. The use of tunable, high brightness synchrotron radiation at micron spatial resolution for x-ray photoelectron spectroscopy provides a technique of choice for mapping the near surface elemental and chemical nature of microstructure in materials. Such a study is essential, for example, for investigation of device failure mechanisms and for the development of next-generation microelectronics devices.

The optical design of the micro-XPS system is such that a spherical mirror accepts 0.2 mrad of monochromatized radiation from a bending magnet beamline with a simple monochromator and focuses the beam to adjustable cross slits, which is the object for the micro-XPS imaging system. The microfocusing is achieved through a pair of orthogonal elliptical bent mirrors (Kirkpatrick-Baez configuration) to focus the beam down to 1 micron x 1 micron. These mirrors are made by bending to steep radii high-strength steel flats polished and edge shaped to high precision [1]. The total flux deliverable at sample location is up to  $2 \times 10^{10}$  photons/s in the energy range from 250 eV to 1500 eV with a resolving power of about 1800. The system has the capability of handling up to 50 mm x 50 mm wafers with an automated 2-stage sample transfer facility. Once the previously fiducialized sample, with laser engraved reference marks, is transferred to the

experimental chamber, it is optically registered using an in-situ optical microscope and the system can also accept particle map information provided from a TENCOR light scattering system. A combination of a precision X-Y stage and laser interferometer encoding allows positioning or scanning of the sample with a precision of 0.1 micron. For XPS study, the photoemitted electrons are energy-analyzed using a PHI electron energy analyzer equipped with a large acceptance angle Omega lens system. The tunability of the synchrotron radiation provides an advantage for carrying out the XPS study using a photon energy chosen to provide a high cross-section for the element of interest and a low cross section for elements whose signal needs to be suppressed. It may also provide some control of depth sensitivity using the kinetic energy dependence of the electron escape depth. The system also incorporates a variety of other instrumentation: standard Al K $\alpha$ /Mg K $\alpha$  x-ray source, a variable energy ion gun for sputtering and depth profiling, and a partial yield electron detector, electron flood gun for sample neutralization (it works best in conjunction with low energy ion source). The same experimental setup allows the carrying out of x-ray absorption studies such as NEXAFS.

The micro-XPS system is fully operational at the ALS. As an example of its application, figure 6 shows a map of a patterned wafer showing bond pads obtained using (a) optical microscope, (b) the corresponding region using Al 2p photoelectrons, and XPS survey scans obtained with the photon beam positioned (c) at the bond pad, and (d) outside the bond pad [2]. The XPS spectrum obtained on the bond pad shows peaks due to fluorine, oxygen, carbon (contaminant) and aluminum. Outside the bond pad one sees peaks due to the substrate silicon and silicon oxide with some traces of fluorine and carbon. Further analysis using curve fitting of high resolution spectra (not shown here) indicates that aluminum is mostly involved in fluorine bonding at the surface.

Figure 6. a) optical image of a patterned wafer (300microns x 400 microns), b) corresponding XPS micrograph image using Al2p photoelectrons, c) XPS survey spectrum at the Al bond pad and d) outside the bond pad.

ALS contact: zhussain@lbl.gov

[1] H.A. Padmore, G. Ackerman, R. Celestre, C-H. Chang, K. Franck, M. Howells, Z. Hussain, S. Irick, S. Locklin, A.A. MacDowell, J.R. Patel, S.Y. Rah, T.R. Renner and R. Sandler, Synchrotron Radiation. News Vol. 10, No 6, 1997, page 18.

[2] i) F. Gozzo et. al., Acta Physica Polonica A **91**, 697 (1997);

ii) F. Gozzo et. al., Proc. Spring Mtg. MRS, San Francisco, April 13-17 (1998)

### **Solar Cell Performance Related to Metal Impurities in Polycrystalline Silicon, Studied with X-ray Fluorescence**

We have directly measured metal impurity distributions in polycrystalline silicon used for terrestrial solar cells. Our goal was to determine whether or not a correlation exists between poorly performing regions of solar cells and metal impurity distributions. Synchrotron-based x-ray fluorescence mapping, with a spatial resolution of 1 mm, was used to measure impurity distributions in polycrystalline silicon at the Center for X-ray Optics, beamline 10.3.1 at the Advanced Light Source [1]. The Light Beam Induced Current method was used to measure minority carrier recombination in order to identify poor performance regions. We have detected iron, chromium and nickel impurities. Figure 7 denotes the spatial distribution of Fe in the scanned region, Cr and Ni were distributed in the same locations as the Fe. The impurity distribution exactly correlated with poor performing regions in the material. These results indicate metal impurities are the cause for high carrier recombination regions in polycrystalline silicon and, therefore,

play a significant role in the performance of the material as a solar cell, as well as yielding insight for methods of solar cell improvement.

Figure 7. Fe distribution in polycrystalline silicon. The Fe distribution exactly correlates with regions of poor solar cell performance.

ALS contact samchugo@lbl.gov

[1] J. H. Underwood, A. C. Thompson, Y. Wu and R. D. Giaque, Nucl. Instr. Meth. A. 266, pg. 318, (1988)

### **Photoemission Microscopy with MAXIMUM**

In 1987, The University of Wisconsin, in collaboration with the Advanced Light Source, began the development of an x-ray microscope system of the scanning type with the goal of reaching a spatial resolution better than 0.1 micron, and a spectral resolution better than 200 meV, working with a base pressure better than  $10^{-10}$  torr. All these goals were achieved in 1992, after a period of development of about 5 years. Several breakthroughs had to be achieved in order to deliver the required performances. In particular, MAXIMUM (Multiple Application X-ray Imaging Undulator Microscope) [1] mounted the first UHV-compatible Schwarzschild objective with in-situ alignment, using for the first at-wavelength Foucault test in extreme ultraviolet (EUV), demonstrating the high efficiency of multilayer optics near the silicon edge.

In the case of MAXIMUM, radiation from the synchrotron source is monochromatized and focused by a Kirkpatrick-Baez (KB) system to illuminate a pinhole, which serve as source for the microscope optics. A multilayer coated (Ru-B<sub>4</sub>C at 130 eV) Schwarzschild Objective (SO) produce an image of the pinhole with a 20x demagnification. When a sample is placed at the focus, photoelectrons are collected by a cylindrical mirror analyzed (CMA) electron spectrometer. The sample is mounted on a scanning stage, and by rastering the sample it is possible to produce a 2-d photoemission image. The schematic of MAXIMUM is reported in Figure 8.

The photoemission microscope MAXIMUM was originally installed at the Synchrotron Radiation Center (SRC) in Madison, WI. During the period from 1992 to 1995, the microscope was successfully used to study semiconductor surfaces, interfaces, biological samples and organic particles. However, during the operation of the microscope, it become apparent that the microscope performance was severely hampered by the relatively low brightness of Aladdin, which limited the available flux at the microscope's focus and, consequently, the achievable spatial resolution because of signal-to-noise consideration. As a consequence, the experiments at SRC were often forced to operate at a reduced resolution in order to obtain realistic counting rates.

The installation of the microscope on a third-generation light source clearly appeared the only possible solution to this problem. A Participating Research Team (PRT) was formed to move MAXIMUM from Wisconsin to the Advanced Light Source (ALS). The microscope was moved to the ALS in April 1995, and it was preliminary installed on the bend magnet beamline 6.3.2, where the preliminary tests were performed. Here we report the successful installation of MAXIMUM on its final location (beamline 12.0 at the ALS) in 1997. This undulator beamline provides  $1.6 \cdot 10^{14}$  photons/sec at 130 eV.

Figure 9 shows a set of images taken by MAXIMUM in its final location at beamline 12.0. Here we investigate in-situ electromigration (EM) in an Al-Cu line. Extensive void

formation is evident in these images. The morphology of the line is given by the secondary electron image at an electron kinetic energy of 5 eV and the residual aluminum oxide skin in the voids is observed to charge at 42 eV, due to the electrical isolation from the rest of the line. The copper precipitates (arrows) are clearly seen at 122 eV (Cu3d), as well as by the contrast reversal from 48 eV to 50 eV, caused by a shift (of about 0.5 eV) of the aluminum oxide core level in Cu-rich regions.

Figure 8. Layout of MAXIMUM at beamline 12.0 at the ALS

Figure 9. Effects of electromigration on a 5 micron Al-Cu wire. The arrows indicate one of the Cu precipitates.

Contact [cerrina@thor.xraylith.wisc.edu](mailto:cerrina@thor.xraylith.wisc.edu)

[1] C. Capasso, A. K. Ray-Chaudhuri, W. Ng, S. Liang, R. K. Cole, J. Wallace, F. Cerrina, G. Margaritondo, J. H. Underwood, J. K. Kortright, and R. C. C. Perera, *J. Vac. Sci. Technol. A*9, 1248 (1991).

### X-ray Micro-Diffraction

Kirkpatrick Baez (KB) mirrors have been developed in the hard x-ray energy range (2-15 keV) [1]. This has allowed progress in the technique of x-ray micro-diffraction. The chosen problem area that defines the instrumental task appropriate to the capabilities of the ALS is the electromigration problem that affects the semiconductor industry. Electromigration is the physical movement of atoms in aluminum interconnect lines passing current at high electron density (typically in the range of  $10^5$  amp/cm<sup>2</sup>). Significant material movement results in voids that consequently lead to breakage and circuit failure in the metal lines. This problem gets more severe as the line dimensions continue to shrink on integrated circuits. In spite of much effort in this field [2,3], electromigration is not understood in any depth or detail, but is strongly associated with the physical material properties (stress and strain) within the aluminum interconnect material. In addition these aluminum wires are buried in an insulating coating (usually SiO<sub>2</sub>). X-rays are ideally suited to probe these buried metallic wires – the requirement being to establish the metallic grain orientation and strain (by measuring small changes in the d spacing) along the wire length. The aluminum grains are typically of size about a micron. The instrumental task is to carry out x-ray crystallography on micron sized samples.

Regular crystallography usually fixes the photon energy and scans the sample angle. If this were carried out with a micron-sized sample and a micron-sized x-ray probe, the sample and x-ray beam would rapidly become mis-aligned as the sphere of confusion of regular goniometers is typically tens of microns. We have adopted the alternative approach of fixing the sample position and scanning the photon energy. Figure 10 shows the schematic for the experimental setup. It consists of a 4-crystal monochromator (two channel cuts) at a distance of 31m from the bending magnet source, followed by the KB mirrors which focus x-rays onto the sample. Spot sizes achieved to date are 0.8 microns FWHM. Diffracted x-rays from the sample are detected by a x-ray CCD. The monochromator crystals are mounted off-axis, which allows the ability to switch between white and monochromatic light whilst illuminating the same spot on the sample. The procedure for this micro-x-ray diffraction is first to find the sample – this is achieved by illuminating the grain of interest with white light and monitoring the Laue pattern with the sample to CCD geometry shown in Figure 11. A typical Laue image from an aluminum grain on a silicon (100) substrate is shown in Figure 12. The bright symmetric spots are those of the silicon substrate, but if one looks closely, there are several weak

asymmetric spots from those of an aluminum grain mis-oriented with respect to the silicon substrate. Digitally subtracting the silicon spots results in the Laue pattern shown in Figure 13, which can then be indexed. With the spots indexed, the d spacing of the relevant planes can be measured by switching to monochromatic light and determining the photon energy of the individual Laue spots. d-spacings have been measured to 1 part in 10<sup>-3</sup> which confirmed the indexation. To measure strain within the aluminum grain, d-spacing measurements some 10-100 times better are required. This work is underway with the delivery of a new custom-built instrument capable of meeting the angular stability requirements.

Figure 10. Schematic layout of the K-B mirrors and the four-crystal channel-cut monochromator.

Figure 11. Schematic layout of the sample – CCD arrangement.

Figure 12. Laue pattern of a single grain in the aluminum interconnect line with the Laue pattern from the silicon substrate. Time for this exposure was 0.5 sec.

Figure 13. Laue pattern from just the aluminum grain after digitally subtracting the silicon Laue pattern.

- [1] A.A. MacDowell, R. Celestre, C.H. Chang, K. Franck, M.R. Howells, S. Locklin, H.A. Padmore, J.R. Patel, and R. Sandler, *SPIE Proceedings* 3152, 126-135 (1998).
- [2] T. Marieb, P. Flinn, J.C. Bravman, D. Gardner, and et al. *J. App Phys.* 78, 1026-1032 (1995).
- [3] P.C. Wang, G.S. Cargill, and I.C. Noyan, *MRS Proceedings* 375, 247-252 (1995).
- [4] A.A. MacDowell, C.H. Chang, H.A. Padmore, J.R. Patel, A.C. Thompson, Presented at the Material Research Society Meeting, San Francisco, Ca, April 13-17, (1998). Proceeding to be published end of 1998.

### **Micro X-ray Absorption Spectroscopy and Micro X-ray Fluorescence for the Earth and Environmental Sciences**

We have done some initial experiments using high spatial resolution determinations of [1] elemental distribution and [2] chemical specificity, on a test facility at the ALS using the intermediate x-ray energy range (2-15 keV) for the earth and environmental sciences in order to determine project feasibility. The two techniques, X-ray Fluorescence Microscopy (XRFM) and Micro-X-ray Absorption Fine-structure Spectroscopy (XAFS), provide characterization probes on the micron scale [1], and thus the study of highly heterogeneous systems. These probes are ideally suited for the study of a variety of scientific problems in the earth and environmental sciences which previously have not been possible to measure or understand. In addition, the appropriate control of time and experimental conditions will provide mechanistic information and new insight into the interaction of such complex systems. Research areas which could directly benefit from this facility include: transport of nutrients and contaminants in plants and symbiotic systems; phytoremediation and phytostabilization mechanisms; mobilization of nutrients or contaminants by colloids; mechanism of formation and function of biominerals in plants and animals; information about diagenesis, climate change and life forms by the investigation of the latter. Very little detail is known about many of the above systems. This is largely due to the lack of available tools to investigate the systems in their natural environment, using probes that are sufficiently small to investigate the changes on the scale with which they were occurring. We present some initial measurements made on various systems of interest.

The first measurements shown are from an ongoing study, in collaboration with researchers at the Norwegian University of Science and Technology [2], on the ability of particular fungi to hyperaccumulate certain contaminant metals. We are studying live fungi from the top organic layer of surface soils in the forest lands of southern Norway. These soils are substantially contaminated by a variety of heavy metals (Zn, Cu, Pb, Cd). It is known that the fungi take up and retain great quantities of the heavy metals, but little is known of the precise forms in which they are retained, or of the mechanisms of uptake and conversion.

Figure 14 shows an optical micrograph of fungi in its natural state (top left). A 400 x 400 micron area of interest is marked on the image with the zinc elemental fluorescence map from this area (lower left). This map shows that the Zn is localized in very small regions of dimensions of only a few microns. Also included are a zinc XAFS spectrum taken from a 5 micron region of high Zn concentration along with a spectrum a zinc oxalate standard. The signal/noise is sufficiently good to scan some way into the Extended XAFS region, which indicates the potential for extracting structural parameters for this system. In this case a preliminary analysis of the short extended region is consistent with the observation by simple comparison with the very distinctive XAFS from the zinc oxalate standard, that there is a high likelihood that this species is zinc oxalate. In addition, our conclusion supports that of recent work by Sarret et al. [3] which showed, using conventional XAFS, that for zinc sequestered by lichen (a symbiotic microorganism consisting of an algae and a fungi) under similar conditions of contaminant exposure, the dominant product is zinc oxalate.

This experiment demonstrates the capability of making a direct species determination on a very small spatial scale. The results suggest that zinc oxalate is an important intermediate in the retention or conversion of Zn by these fungi in their symbiotic relationship with the trees.

We have made some preliminary measurements to the study of the kinetics of formation of mixed metal hydroxides on the surfaces of various clays. Recent XAFS measurements made at the NSLS in studies by Donald Sparks' group at the University of Delaware made an important contribution to the understanding of metal ion retention in the environment [4][5][6]. It was found that under certain conditions of pH and concentration, nickel forms nickel-aluminum hydroxides on the surfaces of a number of clays. These hydroxides are quite resistant to dissolution and less soluble and thus severely reduce the mobility of Ni in the environment. It is thought that the same behavior will apply to a large number of other metal contaminants; the main criteria being that the ionic radius should be close to that of the aluminum cations.

In the Ni study, XAFS spectra were taken at various reaction times of the clay surface with the Ni ions. Despite the clear conclusion that mixed metal hydroxides were forming, it was unfortunately not possible to interpret XAFS data from the low coverages (below 15 minutes reaction time) since the macroscopic concentration was too low and the XAFS data was too noisy.

XRFM measurements of one of the low coverage structures were made at the ALS. These are shown in figure 15A. It can be seen that some form of Ni aggregation or precipitation is already forming at these short reaction times. It was thus possible to make micro-XAFS measurements on these precipitates, which appeared to be a few microns in size. These data are shown in figure 15B along with data taken using the conventional technique of the longest reaction time (250 hours). These initial data indicate that the precipitates formed at these low coverages are of the same type as those formed at the higher coverages. This suggests that the mixed-metal "binding" of contaminants occurs

close to the onset of adsorption which, in itself, has important implications for metal transport in the environment. More extensive studies are planned [7] to check the reproducibility of these initial results. This particular example shows how, in the case where there is aggregation and thus local concentration on the micron scale, micro-XAFS can be more sensitive than the macroscopic technique and why the parameter describing absorber 'dispersion' is more meaningful than the macroscopic value of the concentration.

The last example concerns the ability to directly speciate metals in soils, the most complex of natural systems. The degree of heterogeneity in soils has precluded any direct measurements of contaminant speciation. The most reliable of speciation measurements to date have been made indirectly, for instance by chemical extraction methods (i.e. by applying a series of chemical reagents to infer how the contaminant is bound within the many mineral and organic components within the soil). These indirect methods generally cause alterations to the true soil-contaminant system in the process of trying to make the measurements and are thus notoriously inaccurate.

Figure 16 shows some XRFM and XAFS measurements, made during test measurements [8] of a contaminated soil sample from Long Island. The optical micrograph shows the area of interest within a sample of soil contaminated by Cr. The area sampled is 80 x 60 microns. Three elemental maps of Fe and Cr are shown as determined by x-ray fluorescence. Fe was measured to get an indication of any correlations in the metal distributions, as Fe and Mn oxides are often considered influential in the binding of heavy metals [9]. It can be seen that there is evidence of some correlation between the location of Fe and that of Cr. As can be seen from the elemental maps, the Cr is highly localized (in a region of a couple of microns in size). Significantly, in the case of Cr we can observe a pre-edge feature which is characteristic of some presence of Cr (VI), which is the oxidation state of greatest concern in terms of its mobility and toxicity.

Speciation using unaltered samples of contaminants in such heterogeneous environments as soil represents one of the most important challenges for environmental analysis. When provided in combination with X-Ray Fluorescence for elemental analysis, we can additionally monitor the elemental associations of species with particular minerals. Along with knowledge of the species, this determination of the mineral association is also of central importance for devising effective remediation strategies.

Figure Captions included on figures.

ALS contact [gmlamble@lbl.gov](mailto:gmlamble@lbl.gov)

- [1] A.A. MacDowell, R. Celestre, C-H. Chang, K. Franck, M.R. Howells, S. Locklin, H.A. Padmore, J.R. Patel and R. Sandler, "Progress towards Sub-Micron X-ray Imaging Using Elliptically Bent Mirrors", *Proc. SPIE*, **3152**, pp.126-135, 1997.
- [2] (i) D.G. Nicholson, A. Moen, B. Bethelsen, E. Steinnes and G.M. Lamble; (ii) D. Nicholson, A. Moen, B. Berthelsen, G.M. Lamble, A.A. MacDowell, R.S. Celestre, H.A. Padmore, ALS Highlights 1997. (iii) G.M. Lamble, D.G. Nicholson, A. Moen and B. Bethelsen, submitted to XAFS X, Chicago, IL, Aug 1998.
- [3] (i) "Mechanisms of Lichen Resistance to Metallic Pollution: An in-situ EXAFS Study". G. Sarret, A. Manceau, D. Cuny, C. Van Haluwyn, M. Imbenotte, S. Derulle, J-L Hazemann, Fourth Int. Conf. Biogeochemistry of Trace Elements. June 23-28, (1997), U.C.Berkeley. (ii) Géraldine Sarret, PhD these, Observatoire De Grenoble et Laboratoire de Geophysique Interne et Tectonophysique (1998).
- [4] Spectroscopic Evidence for the Formation of Mixed-Cation Hydroxide Phases Upon Metal Sorption on Clays and Aluminum Oxides, André M. Scheidegger, Geraldine

- M. Lamble and Donald L. Sparks, *Journal of Colloid and Interface Science* **186**, 118-128 (1997)
- [5] The Kinetics of Nickel Sorption on Pyrophyllite as Monitored by X-ray Absorption Fine Structure (XAFS) Spectroscopy, André M. Scheidegger, Geraldine M. Lamble and Donald L. Sparks, *J. De Physique IV France* **7 c2** 773-775, 1997.
- [6] The Kinetics of Mixed Ni-Al Hydroxide Formation on Clay and Aluminum Oxide Minerals: A Time-Resolved XAFS Study, André M. Scheidegger, Daniel G. Strawn, Geraldine M. Lamble and Donald L. Sparks, *Geochimica et Cosmochimica Acta* (accepted).
- [7] Andreas Scheinost, Robert Gale Ford, Geraldine M. Lamble and Donald L. Sparks (in progress).
- [8] (i) R.J. Reeder, G.M. Lamble, A.A. MacDowell, R.S. Celestre, H.A. Padmore, *ALS Highlights 1997*; (ii) Ongoing work with Richard J. Reeder, Department of Earth Sciences, SUNY Stony Brook.

### High Spatial Resolution FTIR Spectromicroscopy

Synchrotron-based infrared (IR) beamlines provide considerable brightness advantages over conventional IR sources [1],[2]. This brightness advantage manifests itself most beneficially when measuring very small samples. In the commissioning of the first IR beamline at the ALS, beamline 1.4.3, we have experimentally measured the small spot-size obtained by our IR microscopy system when using the synchrotron beam as the source and we compare it to the internal Globar source. We demonstrate the resolution-limited focus and the corresponding factor of ~100 improvement over conventional sources in measured signal through very small apertures.

Synchrotron light from the 1.4 bending magnet at the ALS is collimated via a series of aluminum-coated mirrors [3], and is then distributed to one of three end-stations, as schematically drawn in Figure 17. Beamline 1.4.3 inputs the light into a Nicolet Magna 760 purged FTIR spectrometer. The modulated light then passes through a Nic-Plan all-reflecting IR microscope and onto a sample, allowing transmission or reflection measurements throughout the mid-infrared region.

To determine the spot-size at the focus of the IR-microscope, the transmission through a 10 micron aperture was measured as a function of aperture position on the computer-controlled sample stage. This stage has 1 micron spatial resolution, and the FTIR software obtains a spectral map of the transmitted light as a function of x and y position of the stage. No other beam-defining apertures were used. The resultant map of integrated IR intensity versus pin hole position is shown in Figure 18. Cuts of the data along the x- and y-directions result in Gaussian line shapes with widths of 10 mm in x and 8 mm in y. This spot size is becoming diffraction-limited for the low-energy end of our detection capabilities ( $1000\text{ cm}^{-1} = 10\text{ mm}$  wavelength).

When the above synchrotron measurements are compared to analogous measurements made with a conventional Globar IR source, the brightness advantages of the synchrotron become readily apparent. The Globar has a significantly broader peak profile of around 100 mm in width, simply due to the large source size of this glowing filament source, making a better focus impossible. Therefore, while the overall flux from the Globar and the synchrotron sources is comparable, the synchrotron light can be focused onto a 10mm spot. To achieve a similar spot size using the conventional Globar source, one must simply mask the Globar source discarding a large factor of signal intensity. We have measured improvements of several hundred in intensity transmitted through small pin-holes for the synchrotron source compared to the Globar.

Experimental systems where the sample size is quite small, or where features on a sample are on the few micron size scale, will gain significantly by using ALS Beamline 1.4.3. A few examples include observing bacteria ingesting specific chemicals in real time, localization of adsorbates on environmental surfaces, particulate contamination on semiconductors, polymer laminates and composites, analytical forensic studies of small samples, and measuring materials at high pressure in diamond anvil cells. In summary, synchrotron IR spectromicroscopy enables a host of new scientific pursuits where spectral features can be mapped at the few micron spatial scale.

Figure 17. Schematic layout of beamlines 1.4.x at the ALS. 10 by 40 milliradians of synchrotron light from the 1.4 bending magnet port is collected and then collimated in the switchyard. The light is then directed to one of three end-stations which perform UV photoluminescence, vacuum FTIR, and IR spectromicroscopy, respectively.

Figure 18. Integrated IR signal intensity from 2000 - 9000  $\text{cm}^{-1}$  through a 10 mm pin hole being rastered on the IR-microscope stage. There are no other apertures in the optical path. This plot demonstrates the small spot size achieved using the synchrotron IR beam

ALS contact: [mcmartin@lbl.gov](mailto:mcmartin@lbl.gov).

[1] Principal investigators: Michael C. Martin, Wayne R. McKinney and Howard A. Padmore, Advanced Light Source, LBNL.

[2] Hirschmugl, C.J., PhD Thesis Yale University, 1994.

[3] W.R. McKinney, C.J. Hirschmugl, H.A. Padmore, T. Lauritzen, N. Andresen, G. Andronaco, R. Patton, and M. Fong, Proceedings of the SPIE, "Accelerator-Based Infrared Sources and Applications" Volume 3153, pp. 59-67.

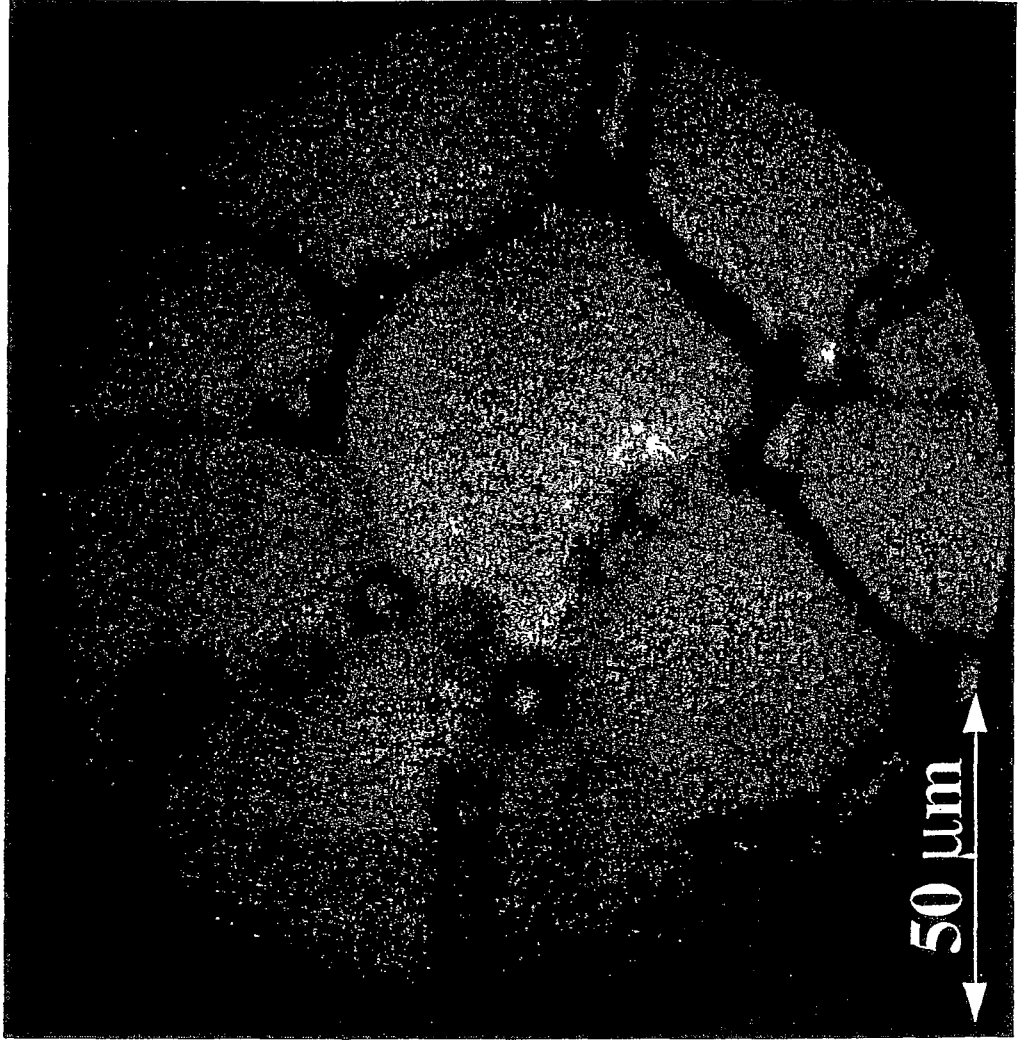


Figure 1

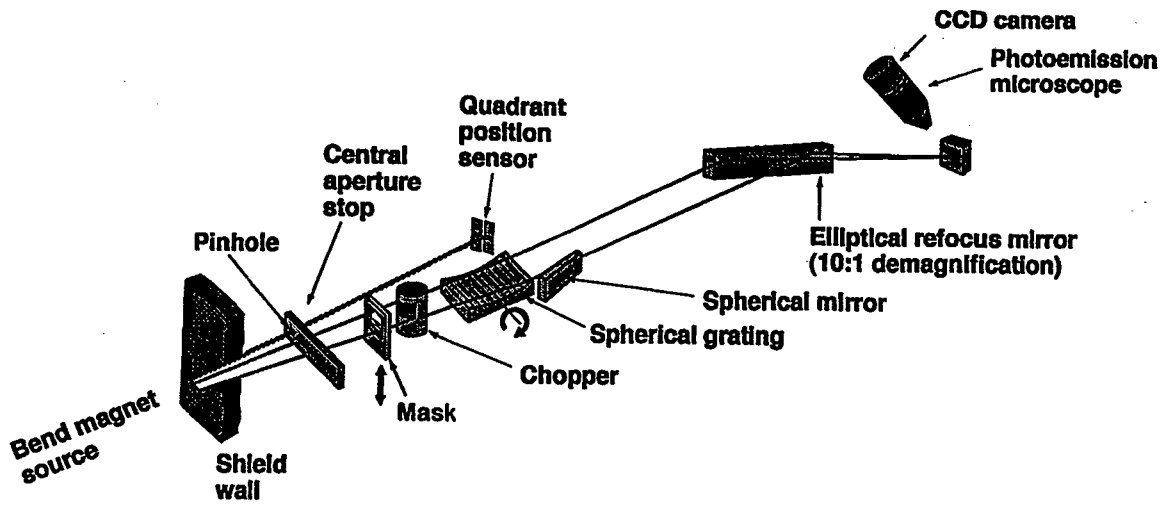


Figure 2

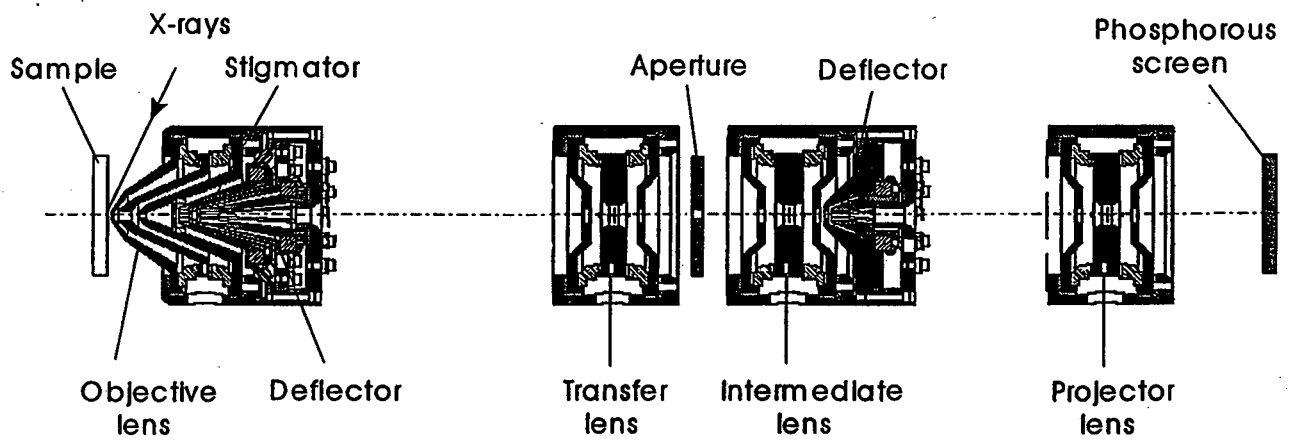
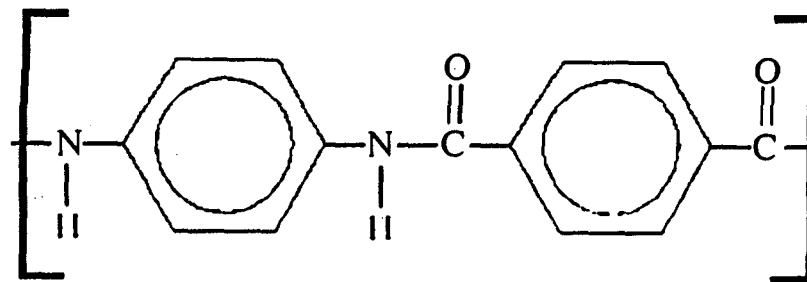
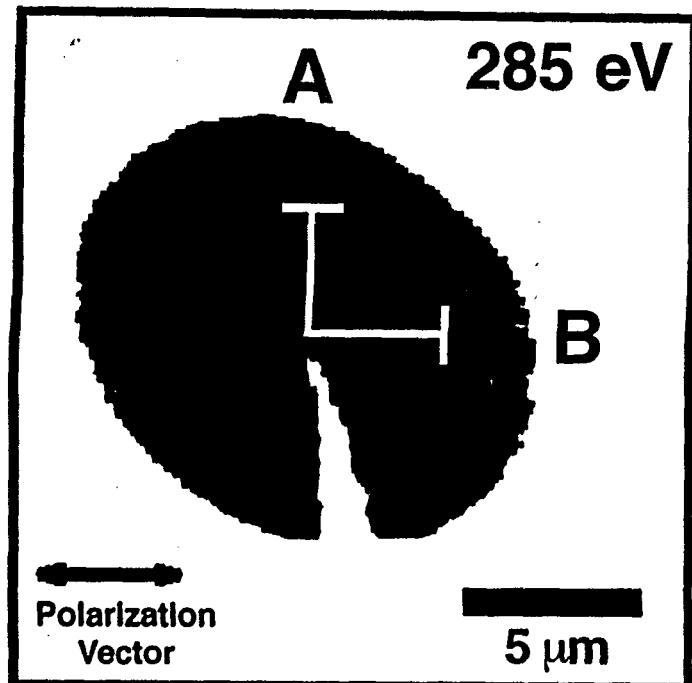
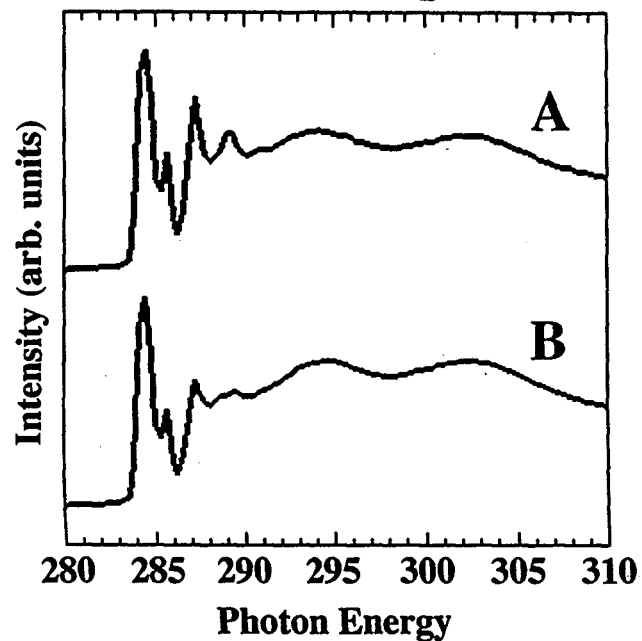


Figure 3

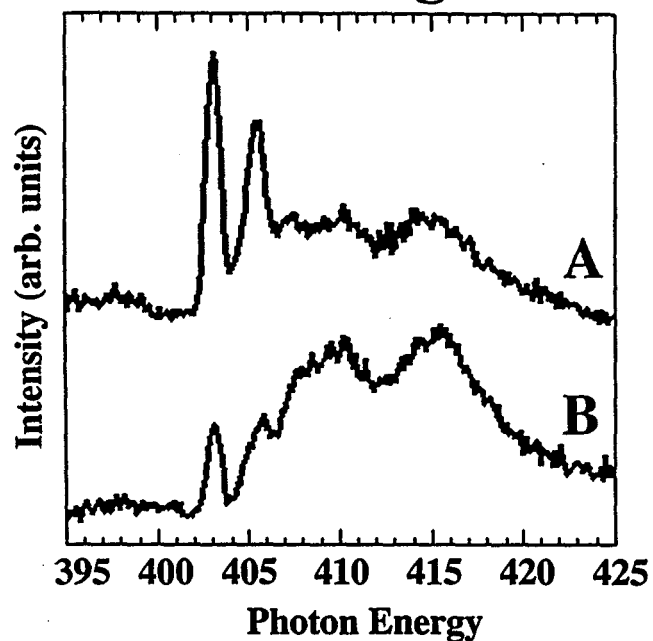


**Kevlar**

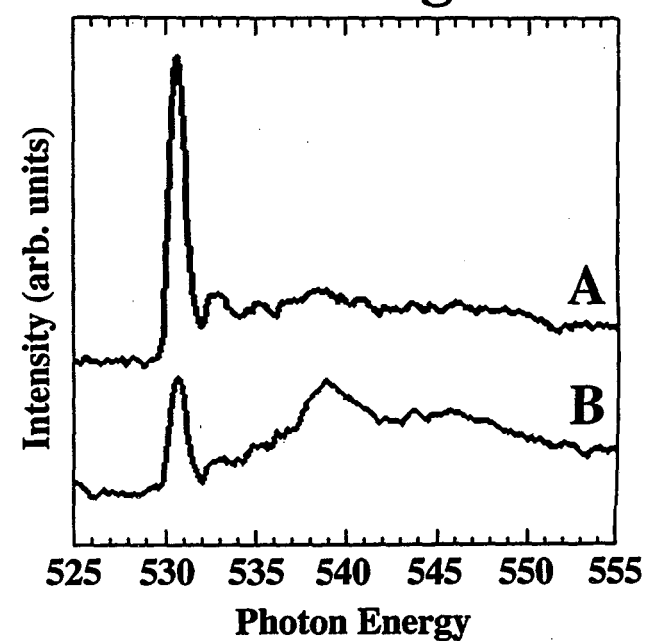
**C K-edge**



**N K-edge**



**O K-edge**



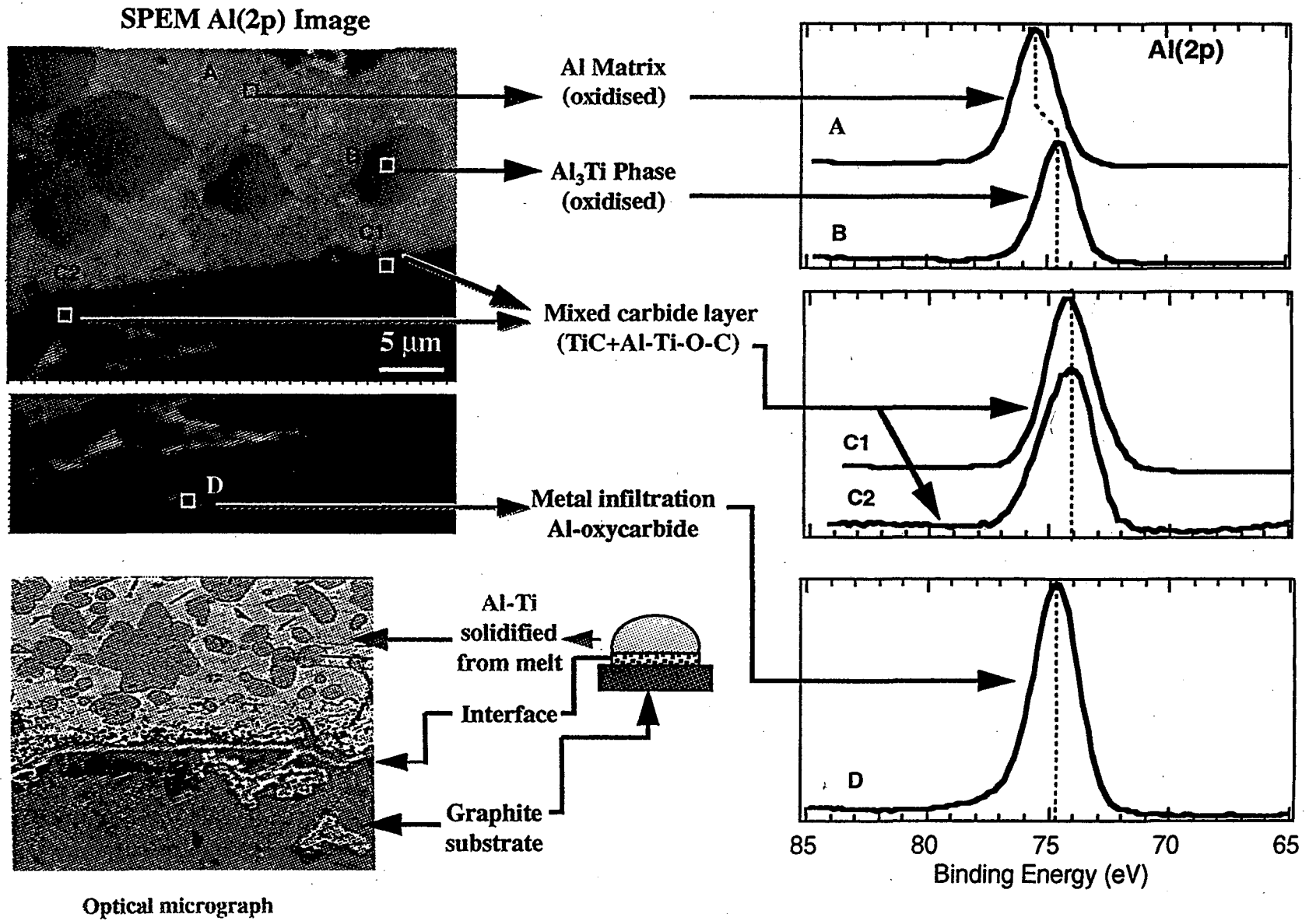


Figure 5

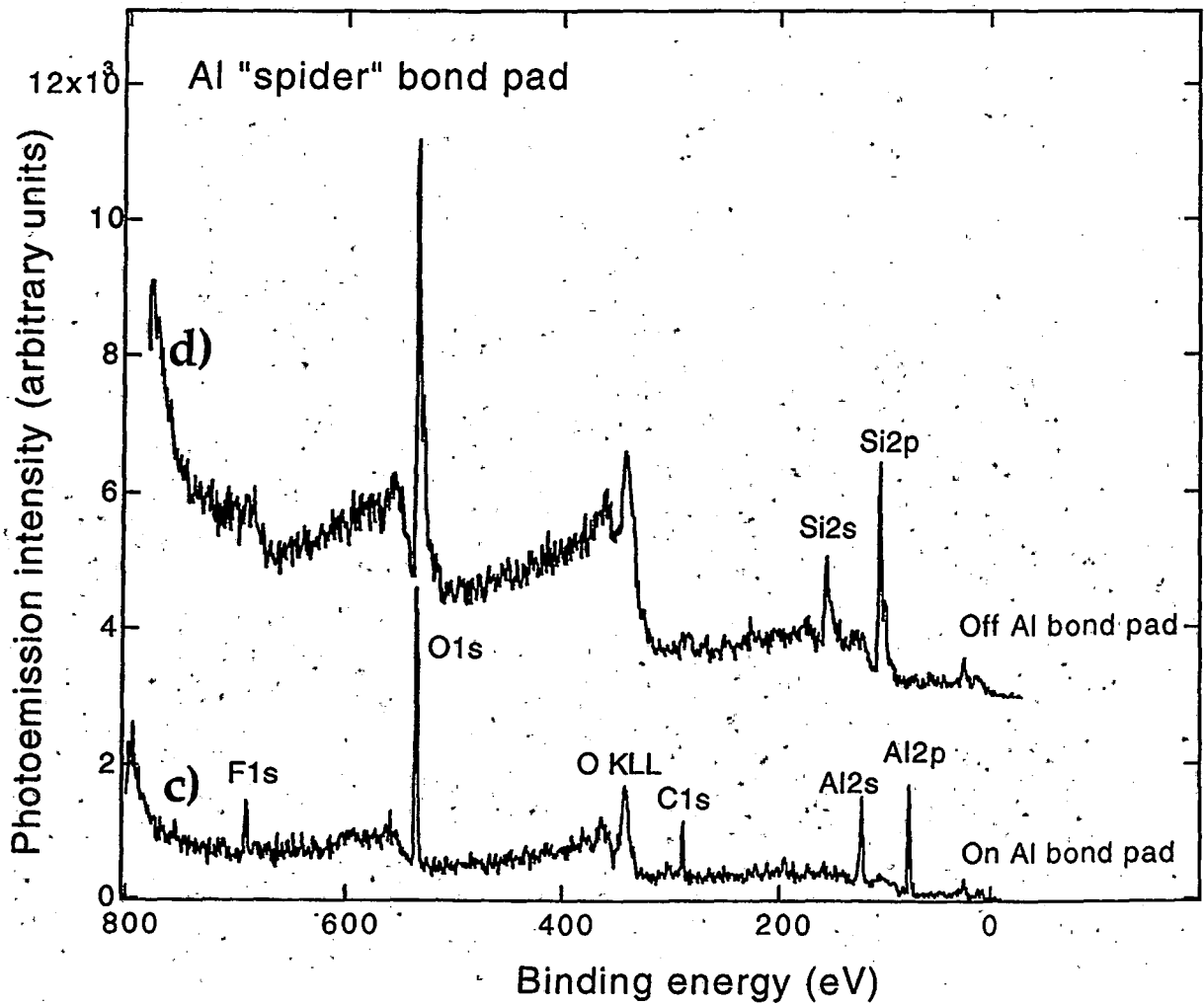
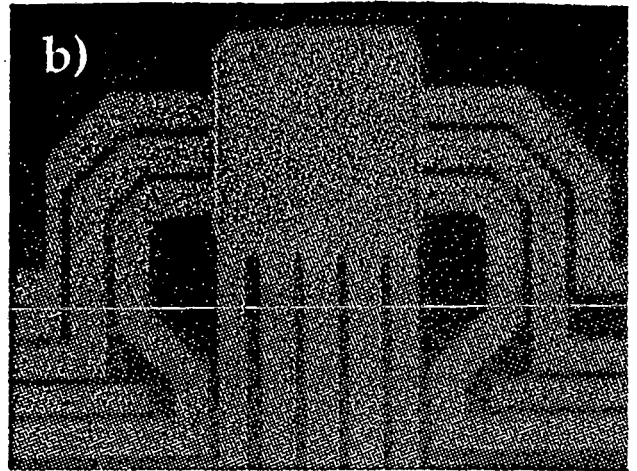
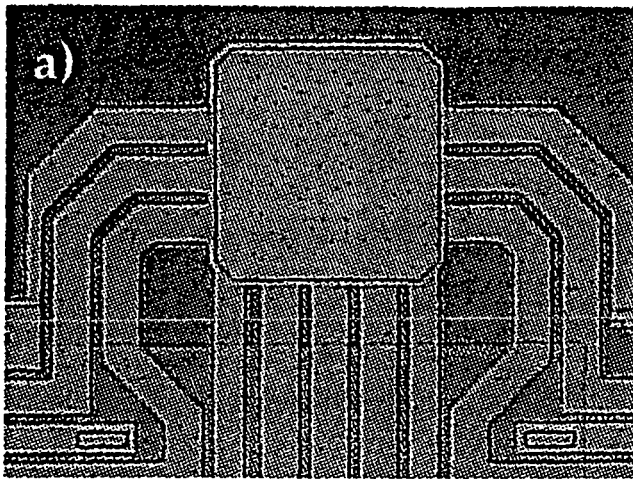


Figure 6.

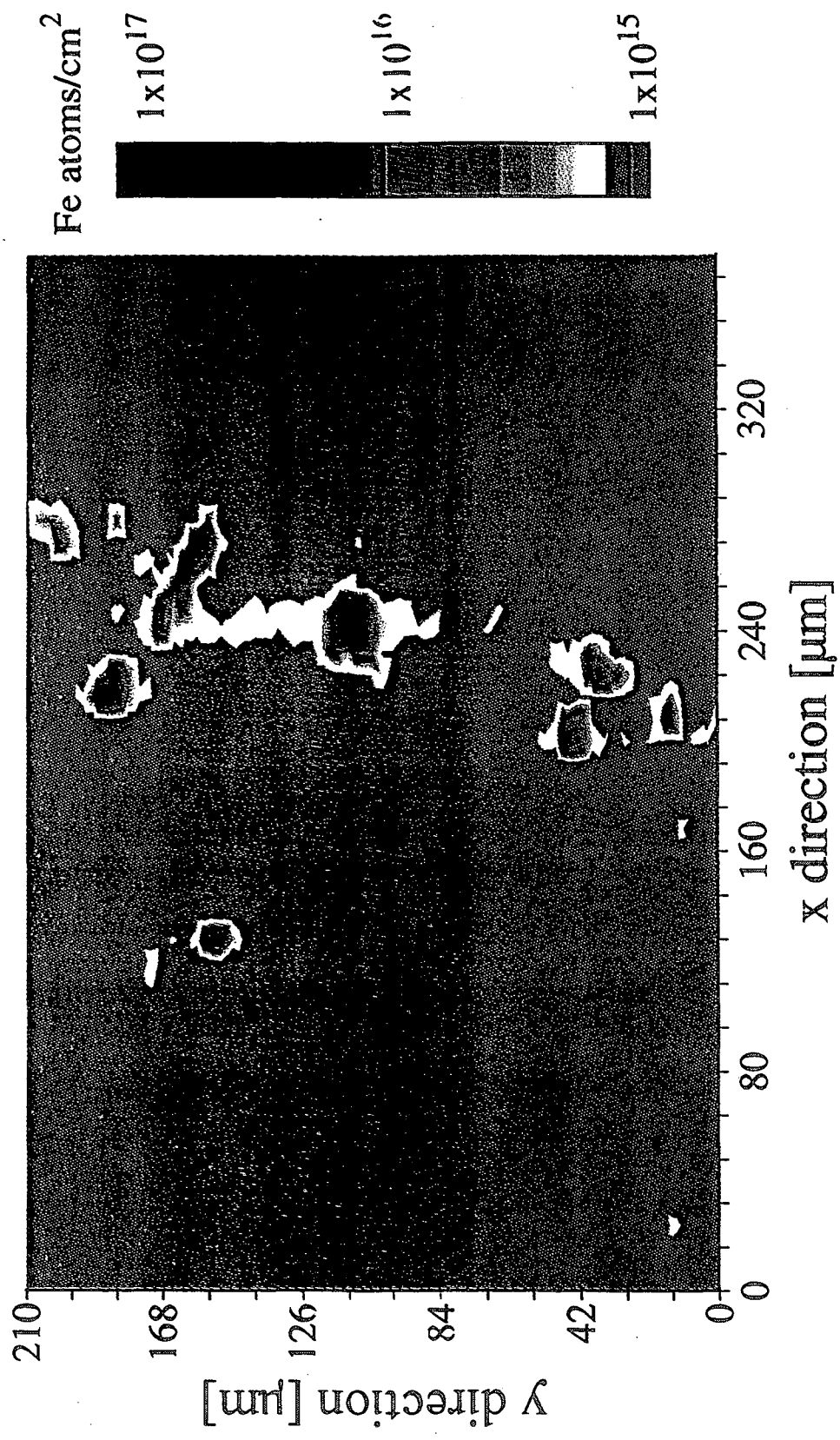


Figure 7

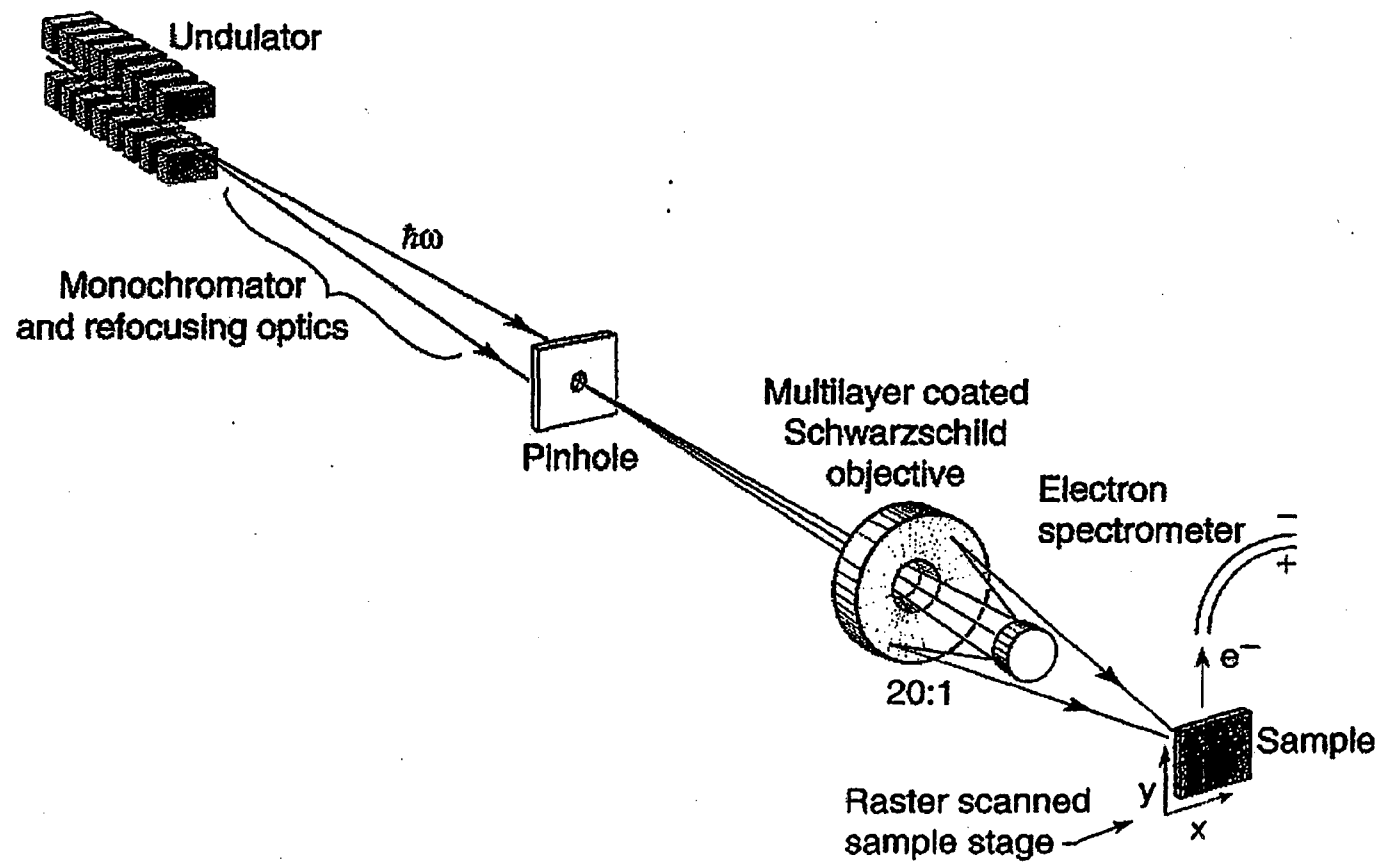


Figure 8

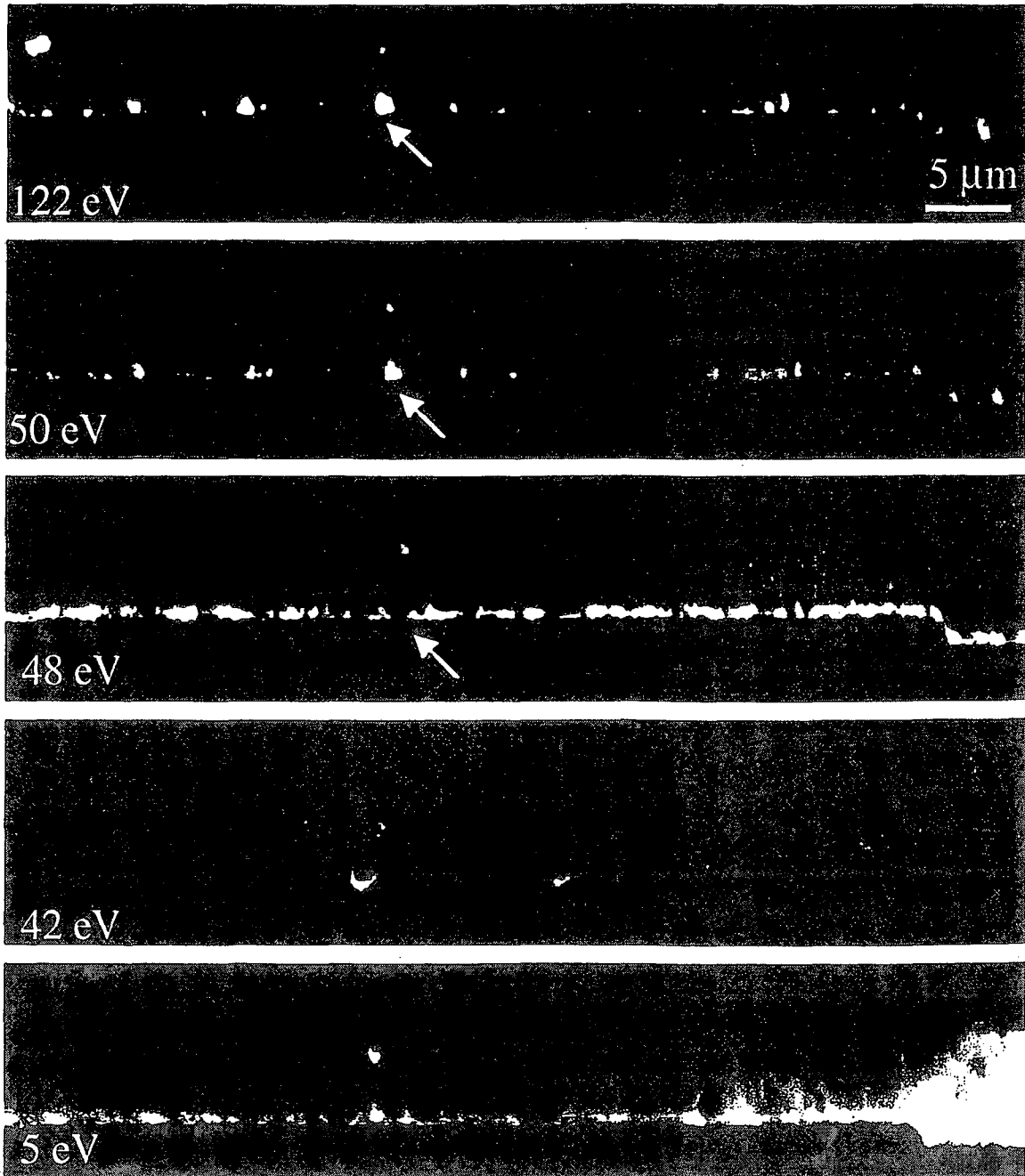


Figure 9

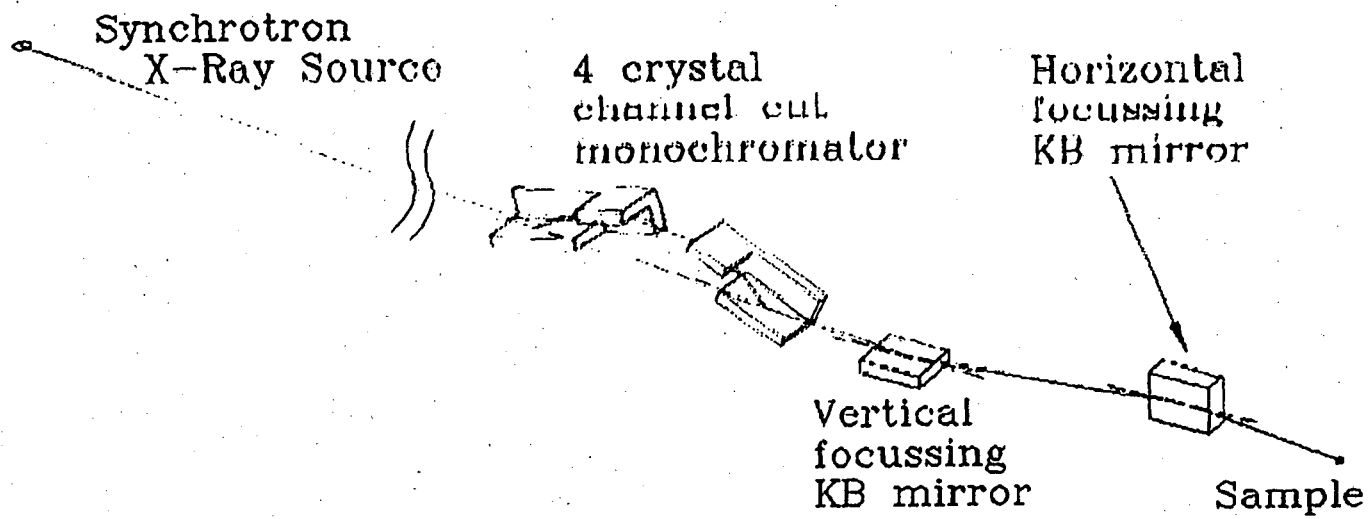


Figure 10

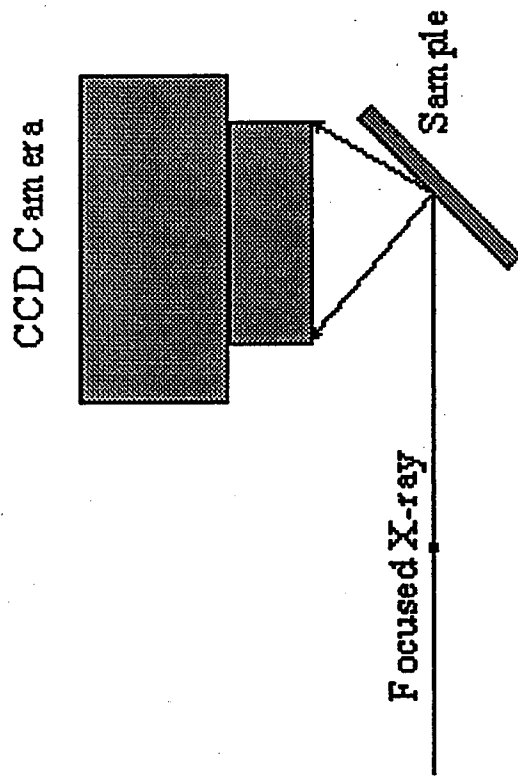


Figure 11

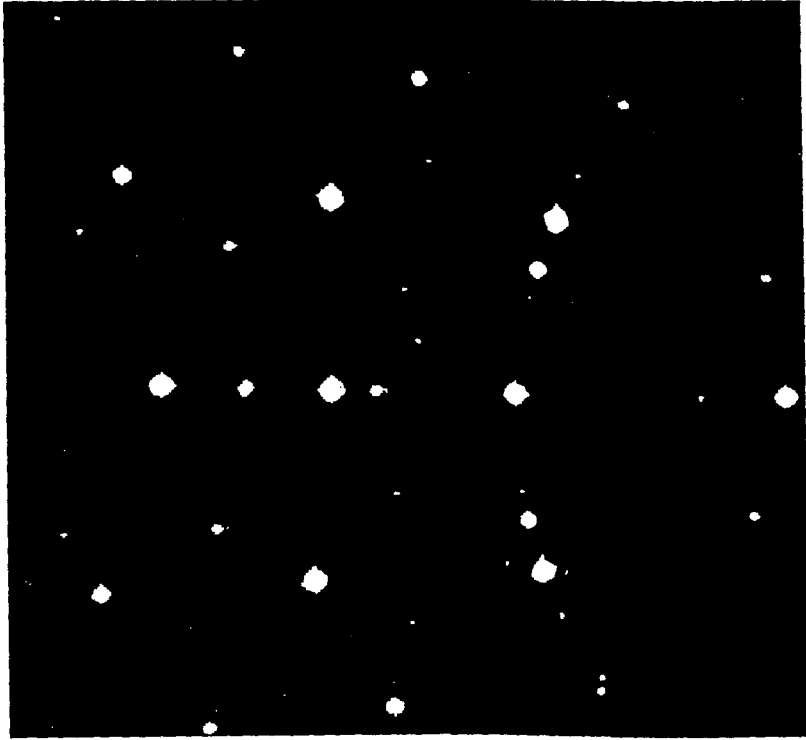


Figure 12

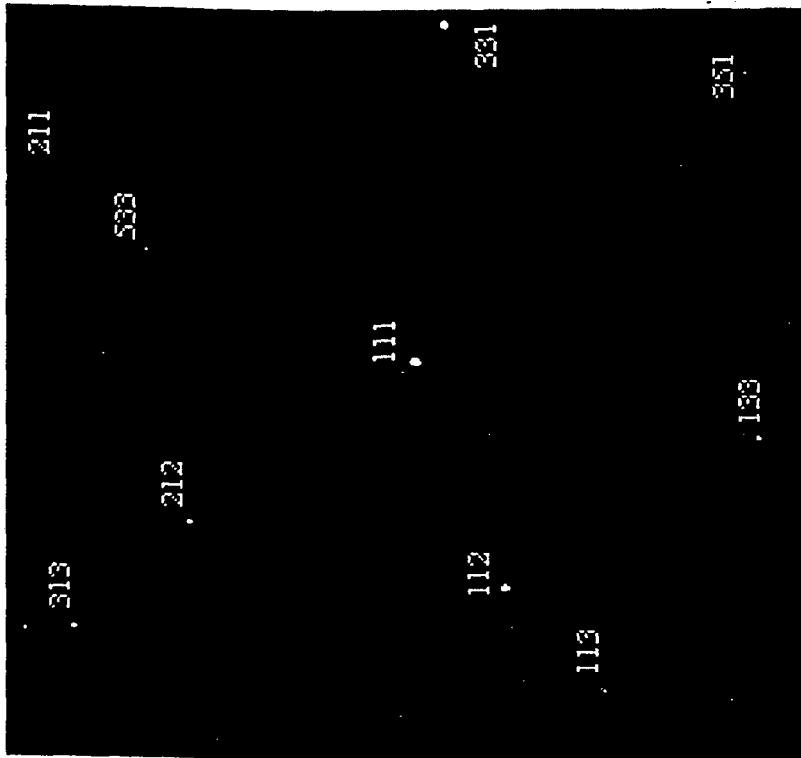
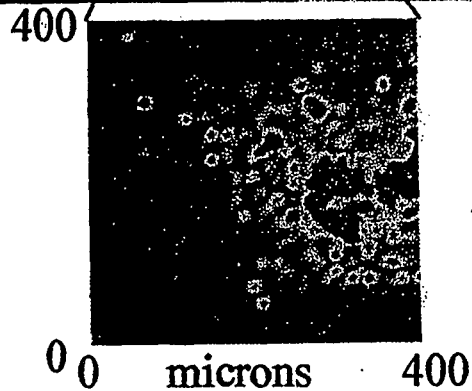
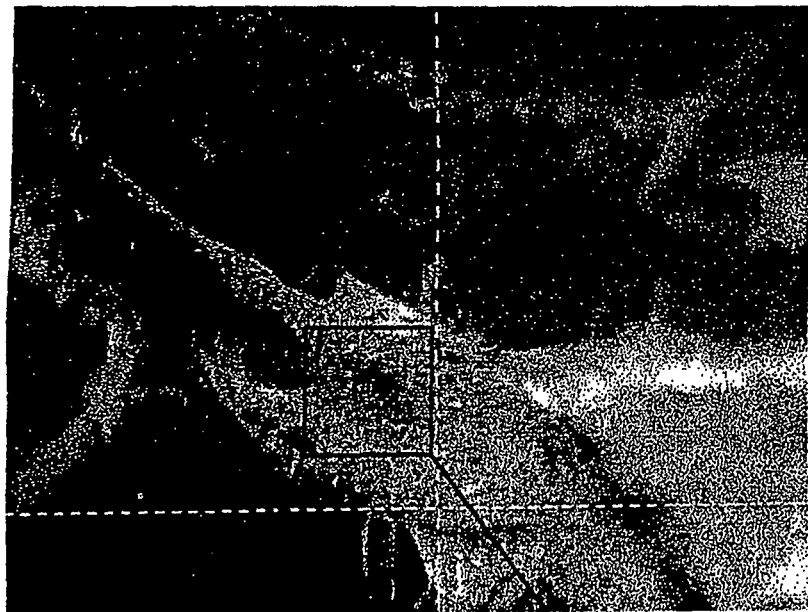


Figure 13

# Zinc Speciation in Fungus from Contaminated Forest Soils



Zinc  
Fluorescence  
Intensity



Micro-XANES of 5um Zinc particle in Fungus  
from contaminated forest soils

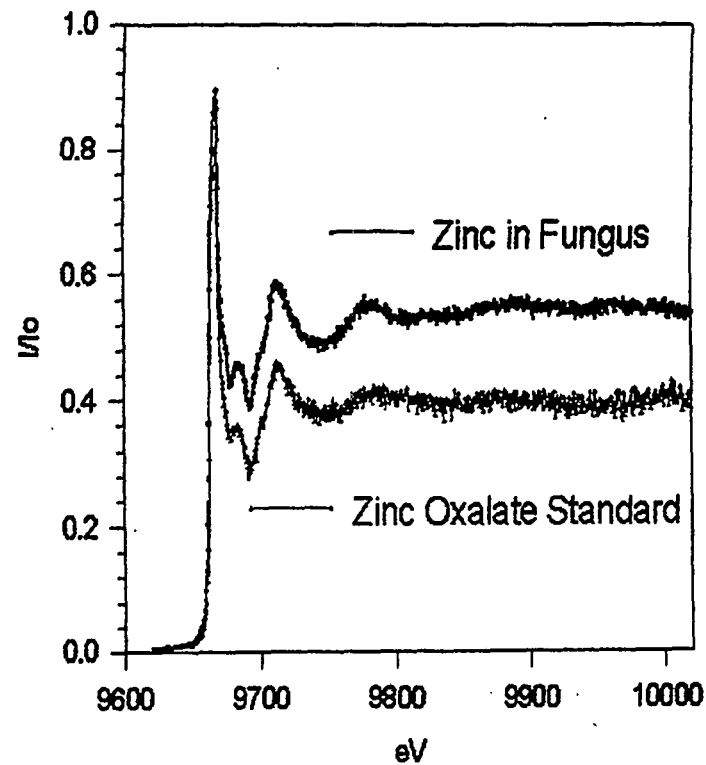
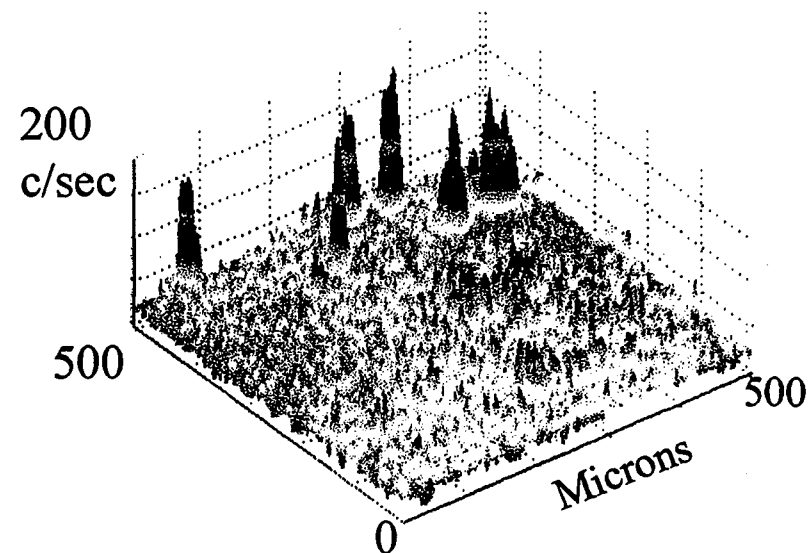


Figure 14

## Ni interaction with clay surfaces after short reaction times

(A) Map of Ni Kedge fluorescence for a low coverage phase (10 minutes reaction time of clay surface with Ni ions) showing regions of local concentration of Ni.



(B)  $\mu$ -XAFS data from initial studies of Ni reaction with clay (pyrophyllite) after short (10 min) reaction time.  $\mu$ -XAFS measured in regions of local concentration as shown in (A).  $\mu$ -XAFS suggests that the precipitates which begin to form at low coverage resemble those at highest metal loadings. This has important implications for considerations of metal transport in the environment.

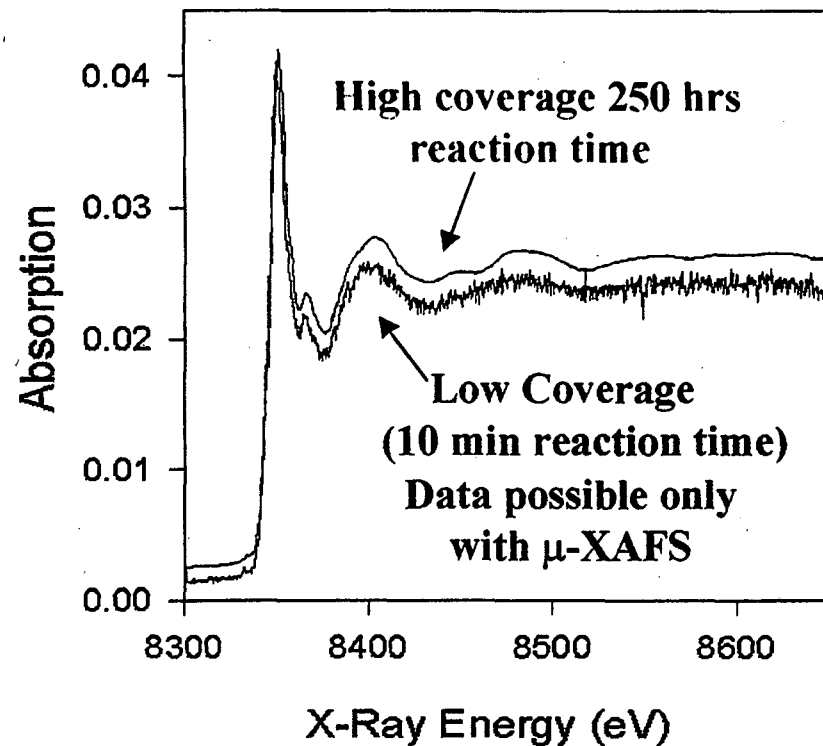


Figure 15

## Speciation of Contaminants in Soil at the micron level

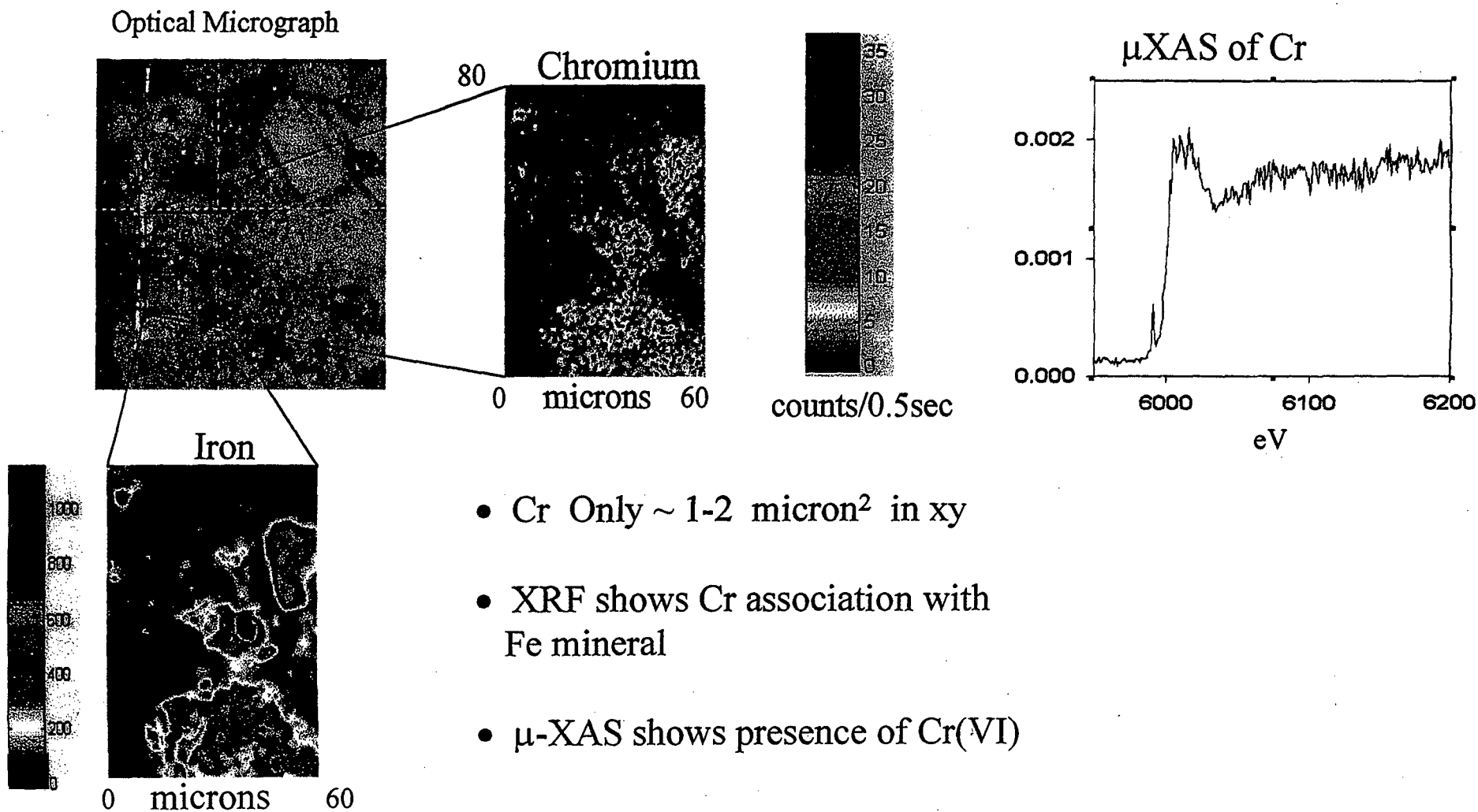


Figure 16

**Beamline 1.4.2 Vacuum FTIR**  
Timing, Surface Science, Bulk Samples

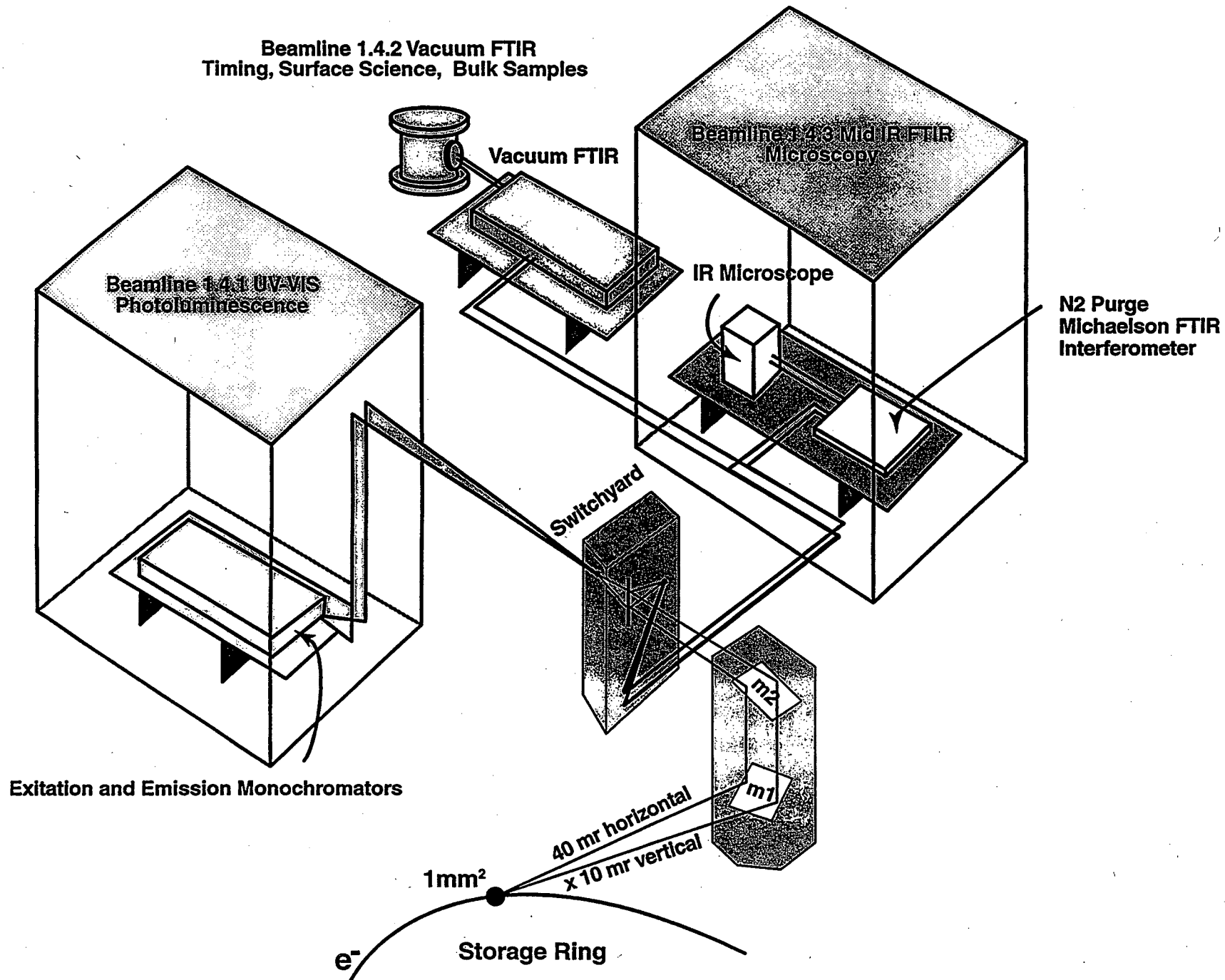
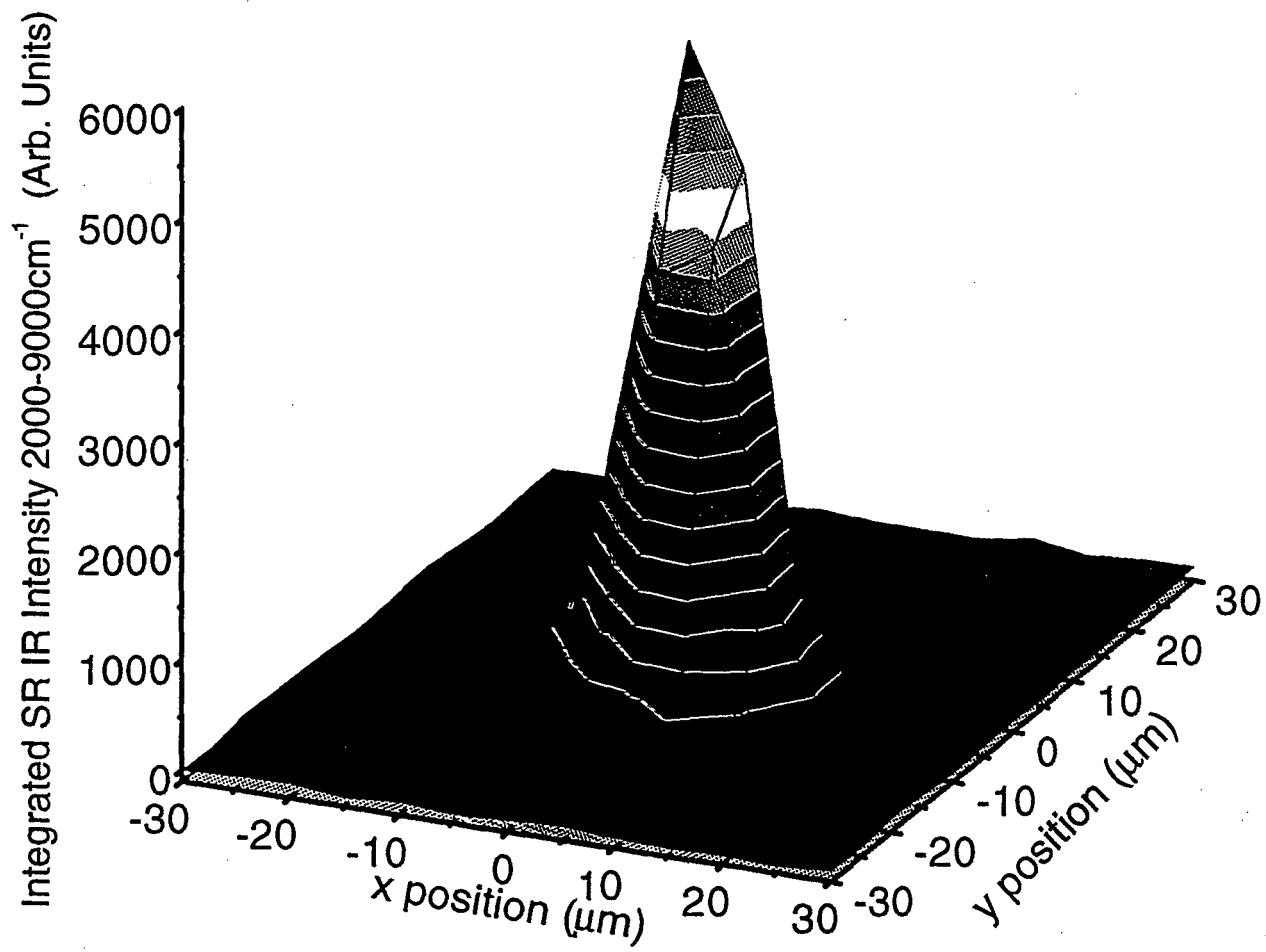


Figure 17



Michael C. Martin, 2/23/98

Figure 18

**ERNEST ORLANDO LAWRENCE BERKELEY NATIONAL LABORATORY**  
**ONE CYCLOTRON ROAD | BERKELEY, CALIFORNIA 94720**

Prepared for the U.S. Department of Energy under Contract No. DE-AC03-76SF00098